Improving breast cancer outcome by preoperative systemic therapy and image-guided surgery

Mieog, J.S.D.

Chapter 10

Antibody-based intraoperative near-infrared fluorescence imaging of primary breast cancer in a syngeneic rat model

Mieog JSD[1], Hutteman M[1], van der Vorst JR, Schaafsma BE, Verbeek FPR, Boonstra MC, Löwik CWGM, Frangioni JV, van de Velde CJH, Kuppen PJK, Vahrmeijer AL

[1] Shared first authorship

ABSTRACT

Introduction

Incomplete tumor resections occur frequently in patients undergoing breast-conserving surgery. Intraoperative near-infrared (NIR) fluorescence imaging is a novel technique to assess the extent of disease during surgery. The current study aimed to investigate whether tumor-targeting monoclonal antibodies conjugated to a NIR fluorescence dye could detect primary breast carcinomas in a syngeneic rat model and be used for image-guided resection.

Methods

The monoclonal mouse antibody MG1, directed against epithelial rat tumor cells, was conjugated to the NIR fluorescent IRDye™800-CW (MG1-CW800) and purified to homogeneity. The isotype-matched irrelevant antibody UPC10 was used as a control. Tumor specificity of MG1-CW800 was assessed using the MCR86 rat breast cancer cell line. *In vivo* tumor targeting was assessed in female WAG/Rij rats carrying EMR86 breast tumors. The Mini-FLARE imaging system was used for intraoperative image-guided resection of EMR86 tumors.

Results

MG1-CW800 bound specifically to MCR86 tumor cells and could identify EMR86 breast tumors in rats using NIR fluorescence. The tumor-to-background ratio (TBR) was highest 24 h after intravenous administration (2.81 ± 0.74). Although UPC10-CW800 did not bound to MCR86 cells, clear tumor demarcation was observed after intravenous injection in EMR86 bearing rats (TBR = 2.95 ± 0.67). Using MG1-CW800, all tumors could be resected under direct image-guidance. MG1-CW800 signal corresponded with histological tumor demarcation.

Conclusion

This study demonstrated that tumor-targeted antibodies conjugated to NIR fluorescence dyes can identify breast tumors in a syngeneic rat model. However, as the control antibody obtained similar *in vivo* results, the 'enhanced permability and retention effect' may be an important factor.

INTRODUCTION

During breast-conserving surgery, the surgeon has to rely on palpation and visual inspection to discriminate tumor tissue from normal tissue. The distinction between tumor and normal tissue is often not evident, resulting in irradical resections in 5 to 40% of patients undergoing breast-conserving surgery, which requires additional resection or intensified radiotherapy regimens.[1-3] Local recurrence rates following breast-conservative therapy of 6.7 to 11% are reported,[4] which can be explained by remnant tumor tissue that is not identified during surgery. Loco regional recurrences are associated with a decrease in overall survival.[4] Therefore, there is a need for a diagnostic tool that can discriminate tumor tissue from normal tissue in real-time during surgery.

Near-infrared (NIR) fluorescence imaging is a technique that has the potential to fulfill this need. NIR light (700 – 900 nm) can penetrate millimeters to centimeters into tissue without the use of ionizing radiation.[5] Several imaging systems have recently become available that are capable of visualizing NIR fluorescence in real-time (reviewed in [6]). Besides these imaging systems, tumor-targeted NIR fluorescent contrast agents ("probes") are necessary to visualize cancer cells. Various mechanisms are available for probes to target tumor cells: they can target increased metabolism,[7] upregulated enzymes,[8-10] or specific cell surface markers.[11] Besides these targeted strategies, a non-targeted approach has been suggested that exploits the so-called 'enhanced permeability and retention (EPR) effect'.[12] The EPR effect is the phenomenon that macromolecules tend to accumulate in tumor tissue much more than they do in normal tissues, which is most probably due to fact that tumors have abnormal 'leaky' neovasculature having endothelial cells with wide fenestrations and lack of smooth muscle layer (Figure 1).

The current study focuses on the use of tumor-targeted antibodies for NIR fluorescence image-guided surgery. Ample clinical experience exists on the use of antibodies in breast cancer, which have been employed for diagnostic imaging,[13, 14] and therapeutic purposes.[15, 16] Moreover, preclinical studies have successfully exploited antibody-based NIR fluorescence tumor targeting.[17, 18] However, these studies were performed in transgenic animal models and lack an adequate isotype-matched control antibody. In this study, we used an antibody directed against epithelial rat tumors, which has been evaluated in a syngeneic rat model of colorectal cancer for the application of immunotherapy and radioimmunotherapy.[19-21] The aim of the current study was to construct an NIR fluorescent tumor-targeted antibody and to validate the intraoperative use of this probe during tumor resection and to compare it with the performance of an isotype-matched irrelevant antibody to control for the EPR effect.

MATERIAL AND METHODS

Animal model

All animals were housed in the animal facility of Leiden University Medical Center. Pellet food and fresh tap water were provided at libitum. The weight of the animals was followed throughout the experiment to monitor their general health state. Throughout imaging and surgical procedures, the animals were anesthetized with inhalation of 2% mixture of isoflurane in oxygen. The Animal Welfare Committee of the Leiden University Medical Center approved the study. The study was conducted in concordance with the "Guidelines for the Welfare of Animals in Experimental Neoplasia" (Second edition, 1997) available online at http://www.ncrn.org.uk/csg/animal_guides_text.pdf.

The EMR86 model is a hormone-dependent, transplantable, metastasizing mammary carcinoma that originated in a female WAG/Rij rat bearing a subcutenously implanted estrogen pellet and has been described previously.[9, 22] EMR86 tumor cells show strong nuclear expression of the estrogen and progesterone receptor, but stain negatively for the human epidermal growth factor receptor 2 (HER2/neu). Therefore, EMR86 tumors closely resemble the luminal A molecular subtype. Orthotopic breast tumors are induced after implantation of fresh EMR86 tumor fragments of 1 mm^3 into the mammary fat pad at four sites in 4 to 6 months old female WAG/Rij rats (Harlan, Horst, The Netherlands) with simultaneous implantation of an estrogen pellet in the intrascapular region of the neck. After four weeks, tumors reach a volume of approximately 1 cm^3, at which time point the experiments were conducted.

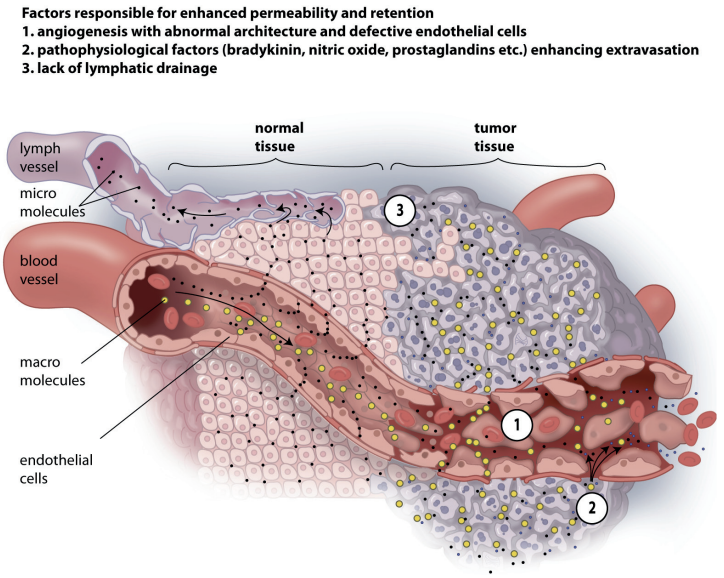

Figure 1. Schematic representation of the 'enhanced permeability and retention effect'.

Immunohistochemistry and *in vivo* homing

MG1 is an IgG2a mouse monoclonal antibody (Antibodies for Research Applications, Gouda, The Netherlands), which originated in Balb/c mice after immunization with CC531 colon adenocarcinoma cells that are syngeneic to WAG/Rij rats.[23] MG1 recognizes an 80 kDa cell surface antigen on rat cancer cells of epithelial origin, with minimal cross-reactivity with other tissues.[23] To assess the specificity of MG1 for EMR86 breast tumors, 4 μm cryosections of snap frozen EMR86 tumors were stained with MG1 as described previously.[23] The IgG2a mouse antibody UPC10 (Sigma Aldrich, Zwijndrecht, The Netherlands), which is directed against β-2-6-linked fructosan, was used as an isotype-matched irrelevant control antibody.[24]

In vivo homing of MG1 to EMR86 tumors was tested by injection of 200 μg of MG1 or UPC10 antibody in 500 μL PBS in the tail vein of EMR86 tumor bearing rats (N = 6 rats, 24 tumors). 24 h after injection, rats were sacrificed and tumors and organs were harvested and snap-frozen on dry ice. Frozen tissue was sectioned and stained as described above, with the exception that no primary antibody was applied.

Construction of NIR fluorescence probes

The NIR fluorescent IRDye 800CW-NHS (LI-COR, Lincoln, NE) was purchased as a dry powder and resuspended to 10 mM in anhydrous dimethyl sulfoxide (DMSO; Sigma Aldrich) under reduced light conditions and stored at -80 °C until used for conjugation.

Preservatives were removed from the solution containing MG1 antibodies using gel filtration chromatography with Zeba spin desalting columns with a cut-off of 7 kDa (Thermo Fisher Scientific, Etten-Leur, The Netherlands). The purified sample was then concentrated using Vivaspin columns (Sigma Aldrich) with a cut-off of 30 kDa and was reconstituted in phosphate-buffered saline (PBS) at pH 7.8. Antibody concentration was estimated using absorbance spectrometry (UltroSpec, Amersham, UK; e_{280nm} = 180,000 M^{-1} cm^{-1}).

IRDye 800CW-NHS was added dropwise to the purified MG1 solution, while maintaining a pH of 7.8. The reactant was gently shaken for 4 h at room temperature. Unreacted dye was separated from conjugated antibodies (MG1-CW800) by gel filtration chromatography with Zeba spin desalting columns with a cut-off of 7 kDa. The labeling ratio of the purified sample was then analyzed using absorbance spectrometry, using the extinction coefficients of MG1 (e_{280nm} = 180,000 M^{-1} cm^{-1}) and CW800 (ε_{785nm} = 240,000 M^{-1} cm^{-1}) in PBS, with correction for 6.5% of measured absorbance at 280 nm of CW800: Ratio = (Abs_{785nm} / ε_{785nm}) / ((Abs_{280nm} – 0.065 * Abs_{785nm}) / e_{280nm}). The same protocol was applied to construct UPC10-CW800.

In vitro confirmation of specificity of MG1-CW800

In vitro cell binding of the newly constructed NIR fluorescent probe MG1-CW800 was tested in the rat breast cancer cell line MCR86, which is recognized by MG1.[23] The characteristics of the cell line and the culture conditions as well as the methods for fluorescence measurements have been described previously.[9] In short, cultured tumor cells were harvested, washed and transferred to a 96-well acrylate plate (Greiner Bio-one, Alphen aan de Rijn, The Netherlands, #655090; suitable for fluorescence measurements). For the binding experiments, 16,000 cells were transferred per well, unless stated otherwise. After 24 h of incubation, cells were washed and MG1-CW800 (6.7 nM to 26.7 nM, 200 µl) was added. In a competitive blocking experiment, unconjugated MG1 was mixed with a fixed MG1-CW800 concentration in order to obtain concentrations of 6.7, 26.7 and 53.4 nM of unconjugated MG1 and 6.7 nM of MG1-CW800, and 200 µl of the mixtures was added to the cells. After incubation of 1 h, cells were washed and fluorescence intensity was measured using the Odyssey NIR fluorescence scanning device (LI-COR, Lincoln, NE). Overlying grids were drawn and integrated intensity was calculated for each well using the Odyssey software (Version 2.1; LI-COR, Lincoln, NE) and corrected for baseline fluorescence signal. UPC10 and UPC10-CW800 were used in a negative control experiment.

In vivo tumor targeting

Tumor bearing rats (N = 14 rats, 55 tumors) were injected into the tail vein with 200 µg of MG1-CW800, UPC10-CW800 or unconjugated IRDye 800CW carboxylate (LI-COR). Rats were imaged at 24 h, 48 h and 120 h after injection of the NIR fluorescent probe using the IVIS Spectrum multispectral imager (Caliper LifeSciences, Hopkinton, MA), which allowed separation of the 800 nm signal from the rat's autofluorescence by means of spectral unmixing. Signal intensity of tumors and surrounding tissue were measured *in vivo*.

Intraoperative NIR fluorescence imaging

Real-time intraoperative NIR fluorescence imaging was performed using the Mini-FLARE imaging system, which has been described previously.[25] Briefly, the system consists of two wavelength isolated light sources: a "white" light source, generating 22,600 lx of 400-650 nm light and a "near-infrared" light source, generating 7.7 mW cm^{-2} of 760 nm light. Color video images and NIR fluorescence images are acquired simultaneously and displayed in real-time using custom optics and software. The system provides the surgeon with real-time images of color video, NIR fluorescence and a pseudocolored merge of the two for anatomical reference.

Image-guided resection

Directed by time optimization experiments, EMR86 tumor bearing rats (N = 6 rats, 24 tumors) were injected with 200 µg of MG1-CW800 via tail vein injection and imaged 24 h thereafter. The Mini-FLARE was positioned at 30 cm above the animal. Guided by the NIR fluorescence images, a skin incision was made and the fluorescent hotspots were resected with a margin of approximately 0.5 cm non-fluorescent tissue. The surgical cavity was inspected for any remnant fluorescence, which, if present, was resected. NIR fluorescence intensity of organs was assessed *in vivo* for biodistribution analyses. Excised tumors were sliced in two parts and snap frozen on dry ice. Tumors were sectioned at 10 µm and air-dried. NIR fluorescence signal was measured using the Odyssey, after which the sections were stained with hematoxylin and eosin.

Statistical analyses

Statistical analyses and generation of graphs were performed using GraphPad Prism software (Version 5.01, La Jolla, CA). Continuous variables were analyzed using the (paired) *t*-test for comparison of two groups. Homogeneity of variance was assessed using Levene's test. Pearson's correlation coefficients *R* were calculated for correlation analyses. All statistical tests were two-tailed and $P < .05$ was considered significant.

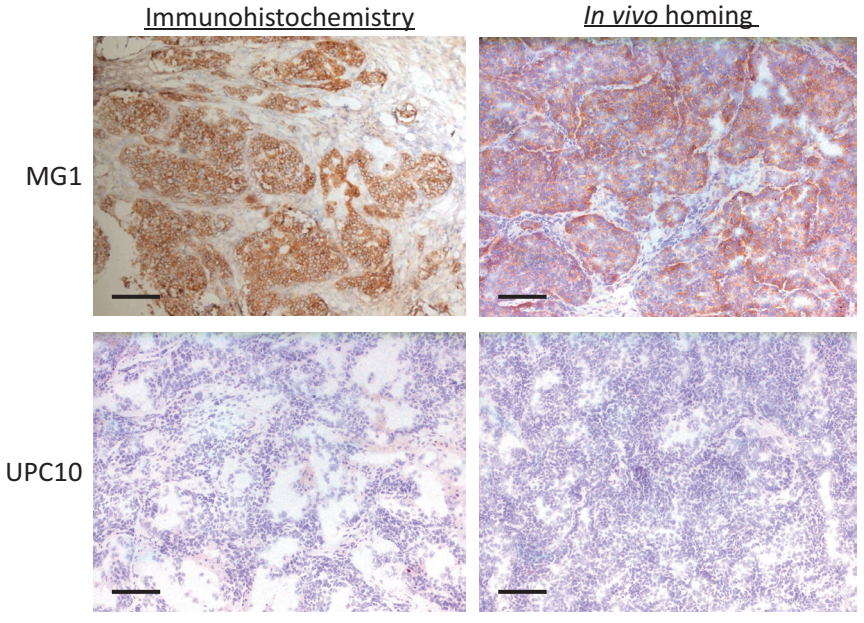

Figure 2. Immunohistochemical confirmation of specificity of MG1 antibodies for EMR86 breast cancer tumors. Incubation of frozen EMR86 sections with MG1 (upper left panel) and UPC10 antibodies (lower left panel). In a homing experiment, rats were intravenously infected with 200 µg MG1 or UPC10 antibody 24 h prior to resection of EMR86 tumors. Staining of frozen sections of these tumors showed presence of MG1 antibodies (upper right panel) and absence of UPC10 antibodies (lower right panel). Bars represent 100 µm.

RESULTS

Specificity of MG1 antibody for EMR86 breast tumors

Cryosections of EMR86 tumors showed clear staining with MG1 after immunohistochemistry and no staining with the UPC10 control antibody (Figure 2). Limited cross-reactivity with other tissues was observed (data not shown), similar to previous results in colorectal cancer.[23] To determine the *in vivo* binding capabilities of MG1 to EMR86 breast tumors, six tumor-bearing rats (N = 24 tumors) were i.v. injected with 200 µg of MG1 or UPC10 antibodies. The tumors were excised 24 h after injection. Immunohistochemical analyses showed adequate homing of the MG1 antibody to the tumors and no homing of the UPC10 antibody (Figure 2).

Construction and *in vitro* testing of NIR fluorescent probes

To construct a NIR fluorescent probe, MG1 antibodies were conjugated to the NIR fluorescent IRDye 800CW. The resulting fluorescent antibody (MG1-CW800) was

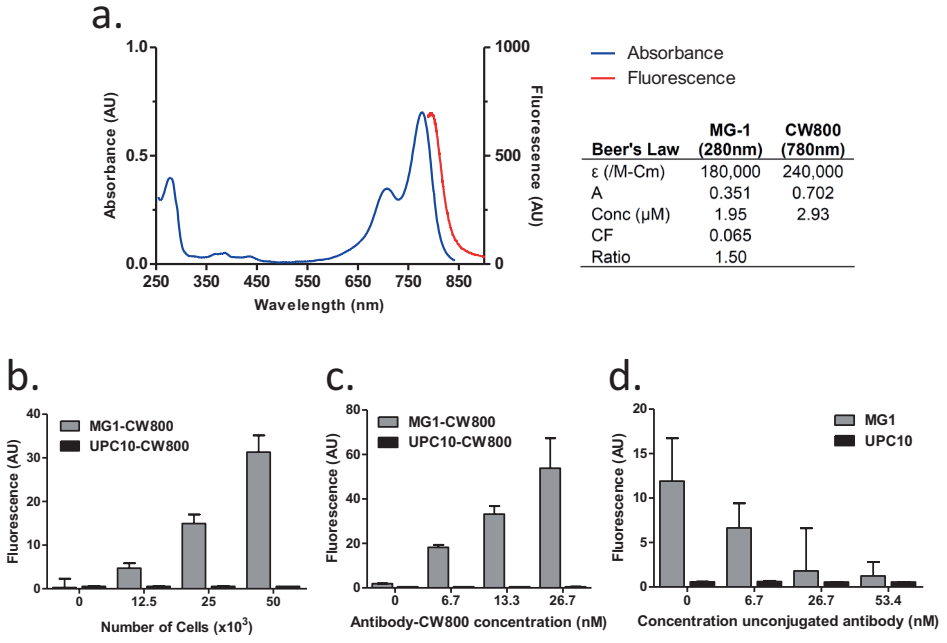

Figure 3. ***In vitro*** **characterization of MG1-CW800. A.** Absorbance and fluorescence spectra of MG1-CW800. Concentration and labeling ratio were determined using Beer-Lambert's law, as shown in the table. **B.** Fluorescence intensity was significantly correlated with the number of MCR86 breast cancer cells ($R = 0.98$, $P < .0001$). **C.** Fluorescence intensity was significantly correlated with the concentration of MG1-CW800 added to a fixed number of MCR86 cells (16,000 cells, $R = 0.95$, $P < .0001$). **D.** Specific binding was demonstrated by linear decrease of fluorescence intensity by adding increasing amounts of unlabeled MG1 ($R = -0.73$, $P = .003$).

separated from reaction products by gel filtration chromatography. The average number of fluorophores per antibody (labeling ratio) as estimated by absorbance spectrometry was 1.6 ± 0.4 (Figure 3A). To test if the binding capacities of MG1-CW800 were retained, cell line experiments were conducted (Figure 3B-D). UPC10-CW800 was used a control NIR fluorescent probe. Fluorescence intensity was significantly associated with number of cells (R = 0.98, P < .0001; Figure 3B) and the concentration of MG1-CW800 (R = 0.95, P < .0001; Figure 3C). Blocking of MG1-CW800 binding to MCR86 tumor cells was performed by adding escalating concentrations of unconjugated MG1. Fluorescence intensity was inversely correlated with the concentration of unconjugated MG1 (R = -0.73, P = .003; Figure 3D). UPC10-CW800 showed no binding with MCR86 cells (Figure 3B-D). These results demonstrated that the specific binding capacities of MG1-CW800 to MCR86 cells were preserved.

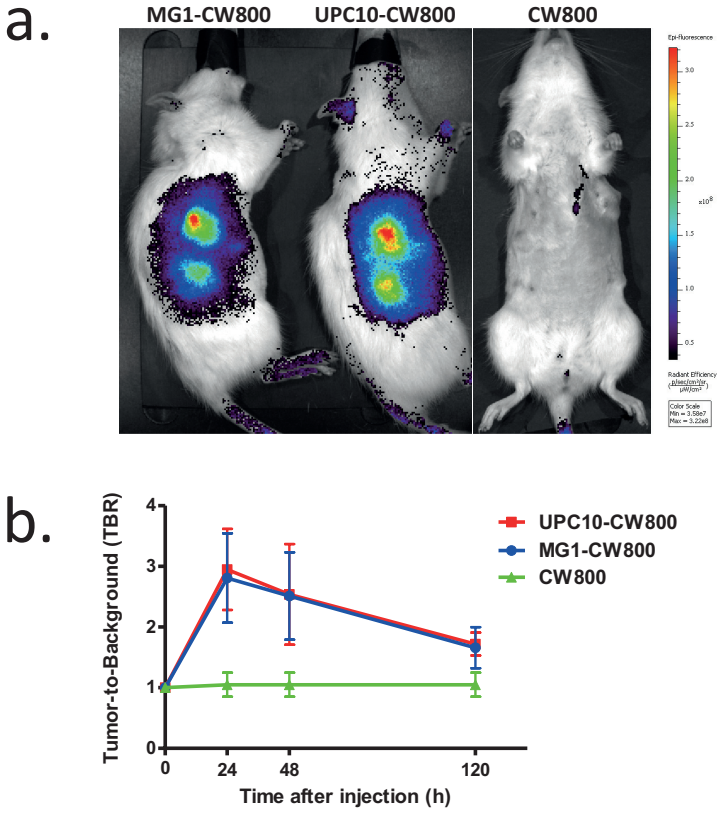

Figure 4. ***In vivo*** **NIR fluorescence detection of EMR86 tumors after intravenous injection of MG1-CW800 or UPC10-CW800. A.** *In vivo* imaging EMR86 tumor-bearing female WAG/Rij rats, 24 h after intravenous administration of 200 µg MG1-CW800 (left), 200 µg UPC10-CW800 (middle panel) or 2 nmol unconjugated IRDye 800CW carboxylate (right panel). Shown is the image after spectral unmixing (IVIS Spectrum). **B.** Tumor-to-background ratios were determined *in vivo* at t = 0, 24 h, 48 h and 120 h after administration of MG1-CW800, UPC10-CW800 and IRDye 800CW carboxylate using the IVIS Spectrum (N = 3 rats in each group).

In vivo tumor targeting NIR fluorescent antibody MG1-CW800

The tumor-targeting properties of the NIR fluorescent antibody MG1-CW800 were tested in the EMR86 breast cancer rat model using the IVIS Spectrum imaging system (Figure 4). Both UPC10-CW800 and unconjugated IRDye 800CW carboxylate were used as a negative control. The tumor-to-background ratio's (TBR) were assessed at 24 h, 48 h and 120 h after injection (Figure 4B). The TBR of rats injected with MG1-CW800 peaked at the 24 h time point and the mean TBR was 2.81 ± 0.74. No significant difference was observed between the 24 h and 48 h time point (t = 1.11, P = .82). Imaging after 120 h resulted in a significantly lower TBR compared to the 24 h time point (t = 4.30, P = .001). Rats injected with UPC10-CW800 showed clear identification of tumors with a mean TBR at 24 h of 2.95 ± 0.67. Rats injected with unconjugated IRDye 800CW carboxylate showed no tumor demarcation. Based on these results, imaging 24 h after administration of fluorescent probe was selected for practical purposes.

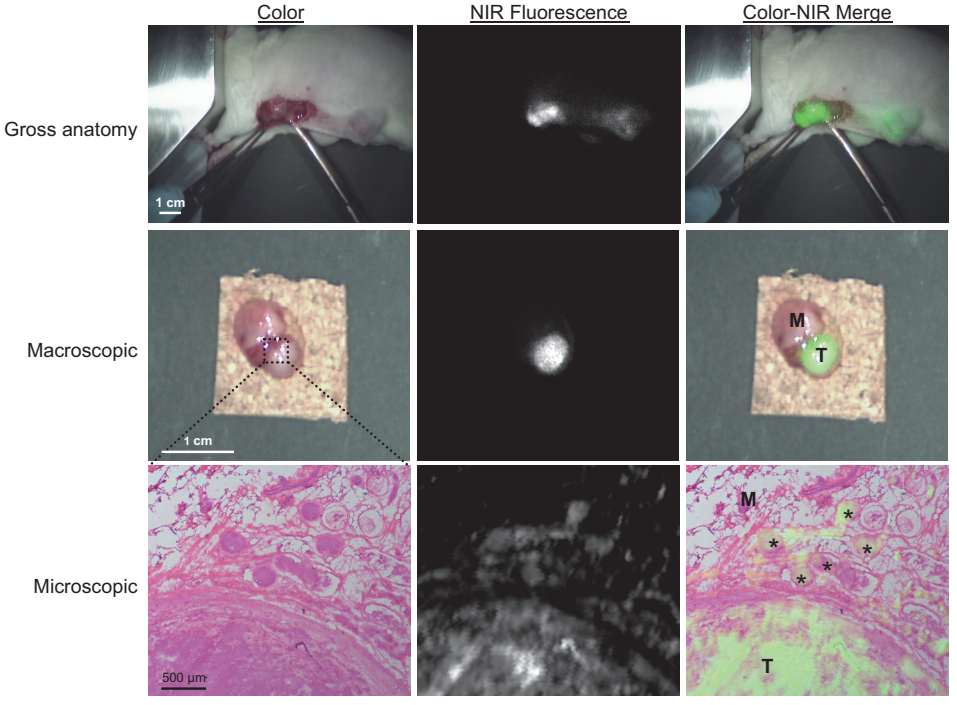

Figure 5. Intraoperative and *ex vivo* tumor identification with NIR fluorescence. Image-guided resection of an EMR86 breast tumor in a rat, 24 h after intravenous administration of 200 µg MG1-CW800 (upper row). Shown are a color image (left panel), NIR fluorescence image (middle panel) and a pseudocolored merge of the two (right panel) as shown in real-time during surgery (Mini-FLARE). *Ex vivo* NIR fluorescence analysis using the Mini-FLARE of resected specimens shows a clear demarcation of the tumor (T) from the surrounding mammary tissue (M; middle row). H&E staining and NIR fluorescence measurement (Odyssey) of cryosections of resected specimens reveal that MG1-CW800 localization corresponds with tumor areas (T = primary tumor, * = tumor satellites) as determined by histology. Surrounding mammary tissue (M) shows no NIR fluorescence (lower row).

Intraoperative NIR fluorescence-guided resection of primary breast cancer

Using the Mini-FLARE intraoperative imaging system, all primary breast tumors (N = 24 tumors, 6 rats) were successfully identified 24 h after intravenous administration of 200 μg MG1-CW800 (Figure 5A). The technique provided a clear demarcation of tumor from surrounding mammary fat pad tissue ($t = 9.95$, $P < .0001$), with an average tumor-to-background ratio of 2.78 ± 0.74. After resection of the primary tumor under direct NIR fluorescence-guidance, no remnant fluorescence hotspots were detected. Histological analyses and fluorescence microscopy (at 800 nm) confirmed that the NIR fluorescent signal of MG1-CW800 corresponded with the presence of tumor cells (Figure 5B-C). In addition, immunohistochemical analysis confirmed that MG1 antibody was present at the cell surface of EMR86 tumor cells (data not shown). Next, the biodistribution of MG1-CW800 was assessed *in vivo* by quantifying the NIR fluorescence signal in selected organs of 6 rats 24 h after intravenous administration of 200 μg MG1-CW800 (data not shown). Because of the renal clearance of the NIR fluorescent probe, the kidney and the bladder showed attenuated fluorescent signal. Most organs, however, showed low fluorescent intensities. Conversely, the liver showed high fluorescence intensity.

DISCUSSION

The current study demonstrated the construction of a NIR fluorescent tumor-targeted antibody (MG1-CW800) and its validation in a syngeneic rat model of breast cancer. *In vitro* characterization showed a linear increase of NIR fluorescence signal with increasing MG1-CW800 concentration and increasing cell concentration. Specificity of the binding was shown *in vitro* by blocking of the NIR fluorescence signal by addition of unlabeled antibody. During the *in vivo* experiments, all breast tumors could be clearly identified by NIR fluorescence after intravenous injection of MG1-CW800. Tumor demarcation as identified by intraoperative NIR fluorescence imaging corresponded to the histological findings.

In vivo, however, animals injected with the NIR fluorescent-labeled UPC10-CW800 isotype control antibody, showed similar tumor uptake as MG1-CW800. As UPC10-CW800 showed no specific binding *in vitro*, the *in vivo* tumor uptake can be attributed to the enhanced permeability and retention effect.[12] Previous studies using radiolabeled UPC10 demonstrated no tumor uptake.[24] The NIR fluorophore used in this study has a molecular weight of 1091 Da, whereas the radiolabel ^{111}Indium has a molecular weight of 111 Da. A recently published study on novel NIR fluorophores has demonstrated the influence of the negative net charge of IRDye 800CW on biodistribution.[26] Future research should focus on the exploiting the effect of size and charge on tumor uptake, whilst minimizing background uptake.

Antibodies are a promising entity to provide contrast during NIR fluorescence image-guided surgery. In contrast to, for example, enzymatic targeting,[27, 28] an antibody targeting the correct antigen will target tumor cells itself, instead of surrounding tissue. Indeed, MG1 has been shown to stain virtually all tumor cells,[23] and similar results have been reported for antibodies against human targets.[29, 30] Several antibodies are available for clinical application,[15, 31, 32] with a multitude in the process of clinical approval. As the first fluorophores, including IRDye 800CW, are in the process of clinical approval,[33] it is expected that combining such a novel fluorophore with an already clinically available tumor-targeting agent (for example trastuzumab, bevacizumab and cetuximab) will encounter less roadblocks from bench to bedside.[34] Moreover, as these antibodies are already employed for novel adjuvant treatment options, as immunotherapy,[15, 31] radioimmunotherapy,[35] or pretargeted radioimmunotherapy,[36, 37] these antibodies have the potential to be used for both intraoperative tumor visualization and perioperative treatment of residual disease.

For an optimal tumor demarcation using NIR fluorescence probes, tumor binding needs to be maximized, while minimizing background uptake.[38] Therefore, an optimal tumor-targeting NIR fluorescent probe has a high affinity for the targeted ligand, has low non-specific uptake in non-targeted tissue, and unbound molecules are cleared rapidly from the body.[39] Antibodies as MG1 have a molecular weight of approximately 150 kDa and are therefore macromolecules, which have a relatively long blood half-life of 330 minutes.[40] In the current study, a high NIR fluorescence signal was observed in the liver, which could be caused by specific binding of the Fc region of the antibody and subsequent degradation of the immune complex by Kuppfer cells,[41] or aspecific binding by the liver parenchyma due to the surface charge and hydrodynamic diameter of MG1-CW800. Although the uptake in the liver would not directly hamper the ability to demarcate breast tumors (as opposed to intra-abdominal tumors, where this could be a significant impairment[42]), lower aspecific uptake will decrease the required dose and reduce potential side effects. Therefore, future studies will have to focus on smaller tumor-targeted entities (e.g. peptides,[43, 44] peptidomimetic molecules,[45-47] or antibody fragments[48]) that should be combined with optimized fluorophores, with minimal background uptake, to optimize biodistribution and clearance properties in order to maximize contrast with minimal dosing.[39]

In conclusion, this study shows the tumor-targeting capabilities of a newly constructed NIR fluorescent antibody and its use for intraoperative tumor demarcation of breast tumors, in a preclinical animal model. An aspecific isotype control antibody demonstrated similar *in vivo* tumor uptake, indicating the influence of the enhanced permeability and retention effect. The use of an antibody based tumor-targeting strategy permits the use of currently clinically available molecules, could enable combined use for visualization and treatment and therefore has the potential to be translated to the clinic in the foreseeable future.

ACKNOWLEGDEMENTS

This work was supported in part by the Dutch Cancer Society grant UL2010-4732 and the Center for Translational Molecular Medicine (DeCoDe project, grant 03O-101). J.S.D. Mieog is a MD-medical research trainee funded by The Netherlands Organisation for Health Research and Development (grant nr. 92003526). We want to thank Rob Keyzer, Gabi van Pelt, Karien de Rooij and Isabel Mol for technical assistance and Lindsey Gendall for editing.

REFERENCES

1. Verkooijen HM, Borel RI, Peeters PH, et al. Impact of stereotactic large-core needle biopsy on diagnosis and surgical treatment of nonpalpable breast cancer. Eur J Surg Oncol 2001; 27:244-9.
2. Mai KT, Yazdi HM, Isotalo PA. Resection margin status in lumpectomy specimens of infiltrating lobular carcinoma. Breast Cancer Res Treat 2000; 60:29-33.
3. Rizzo M, Iyengar R, Gabram SG, et al. The effects of additional tumor cavity sampling at the time of breast-conserving surgery on final margin status, volume of resection, and pathologist workload. Ann Surg Oncol 2010; 17:228-34.
4. Clarke M, Collins R, Darby S, et al. Effects of radiotherapy and of differences in the extent of surgery for early breast cancer on local recurrence and 15-year survival: an overview of the randomised trials. Lancet 2005; 366:2087-106.
5. Frangioni JV. In vivo near-infrared fluorescence imaging. Curr Opin Chem Biol 2003; 7:626-34.
6. Gioux S, Choi HS, Frangioni JV. Image-guided surgery using invisible near-infrared light: fundamentals of clinical translation. Mol Imaging 2010; 9:237-55.
7. Zhou H, Luby-Phelps K, Mickey BE, et al. Dynamic near-infrared optical imaging of 2-deoxyglucose uptake by intracranial glioma of athymic mice. PLoS One 2009; 4:e8051.
8. Weissleder R, Tung CH, Mahmood U, et al. In vivo imaging of tumors with protease-activated near-infrared fluorescent probes. Nat Biotechnol 1999; 17:375-8.
9. Mieog JS, Hutteman M, van der Vorst JR, et al. Image-guided tumor resection using real-time near-infrared fluorescence in a syngeneic rat model of primary breast cancer. Breast Cancer Res Treat 2011; 128:679-89.
10. Jiang T, Olson ES, Nguyen QT, et al. Tumor imaging by means of proteolytic activation of cell-penetrating peptides. Proc Natl Acad Sci USA 2004; 101:17867-72.
11. Backer MV, Levashova Z, Patel V, et al. Molecular imaging of VEGF receptors in angiogenic vasculature with single-chain VEGF-based probes. Nat Med 2007; 13:504-9.
12. Iyer AK, Khaled G, Fang J, et al. Exploiting the enhanced permeability and retention effect for tumor targeting. Drug Discov Today 2006; 11:812-8.
13. Dijkers EC, Oude Munnink TH, Kosterink JG, et al. Biodistribution of 89Zr-trastuzumab and PET imaging of HER2-positive lesions in patients with metastatic breast cancer. Clin Pharmacol Ther 2010; 87.
14. Oude Munnink TH, Nagengast WB, Brouwers AH, et al. Molecular imaging of breast cancer. Breast (Edinburgh, Scotland) 2009; 18 Suppl 3.
15. Hudis CA. Trastuzumab-mechanism of action and use in clinical practice. N Engl J Med 2007; 357:39-51.
16. Giampaglia M, Chiuri VE, Tinelli A, et al. Lapatinib in breast cancer: clinical experiences and future perspectives. Cancer Treat Rev 2010; 36 Suppl 3.
17. Ballou B, Fisher GW, Waggoner AS, et al. Tumor labeling in vivo using cyanine-conjugated monoclonal antibodies. Cancer immunology, immunotherapy: CII 1995; 41:257-63.
18. Ballou B, Fisher GW, Deng JS, et al. Cyanine fluorochrome-labeled antibodies in vivo: assessment of tumor imaging using Cy3, Cy5, Cy5.5, and Cy7. Cancer Detect Prev 1998; 22:251-7.

19. de Jong G, Hendriks T, Franssen G, et al. Adjuvant radioimmunotherapy after radiofrequency ablation of colorectal liver metastases in an experimental model. Eur J Surg Oncol 2011; 37:258-64.
20. de Jong GM, Hendriks T, Eek A, et al. Adjuvant radioimmunotherapy improves survival of rats after resection of colorectal liver metastases. Ann Surg 2011; 253:336-41.
21. Gelderman KA, Hakulinen J, Hagenaars M, et al. Membrane-bound complement regulatory proteins inhibit complement activation by an immunotherapeutic mAb in a syngeneic rat colorectal cancer model. Mol Immunol 2003; 40:13-23.
22. Wijsman JH, Cornelisse CJ, Keijzer R, et al. A prolactin-dependent, metastasising rat mammary carcinoma as a model for endocrine-related tumour dormancy. Br J Cancer 1991; 64:463-8.
23. Hagenaars M, Koelemij R, Ensink NG, et al. The development of novel mouse monoclonal antibodies against the CC531 rat colon adenocarcinoma. Clin Exp Metastasis 2000; 18:281-9.
24. de Jong GM, Hendriks T, Eek A, et al. Radioimmunotherapy improves survival of rats with microscopic liver metastases of colorectal origin. Ann Surg Oncol 2009; 16:2065-73.
25. Mieog JS, Troyan SL, Hutteman M, et al. Towards optimization of imaging system and lymphatic tracer for near-infrared fluorescent sentinel lymph node mapping in breast cancer. Ann Surg Oncol 2011; 18:2483-91.
26. Choi HS, Nasr K, Alyabyev S, et al. Synthesis and in vivo fate of zwitterionic near-infrared fluorophores. Angewandte Chemie 2011.
27. Bogyo M. Finding enzymes that are actively involved in cancer. Proc Natl Acad Sci USA 2010; 107:2379-80.
28. Kirsch DG, Dinulescu DM, Miller JB, et al. A spatially and temporally restricted mouse model of soft tissue sarcoma. Nat Med 2007; 13:992-7.
29. Packeisen J, Kaup-Franzen C, Knieriem HJ. Detection of surface antigen 17-1A in breast and colorectal cancer. Hybridoma 1999; 18:37-40.
30. Gottlinger HG, Funke I, Johnson JP, et al. The epithelial cell surface antigen 17-1A, a target for antibody-mediated tumor therapy: its biochemical nature, tissue distribution and recognition by different monoclonal antibodies. Int J Cancer 1986; 38:47-53.
31. Rini BI. Vascular endothelial growth factor-targeted therapy in renal cell carcinoma: current status and future directions. Clin Cancer Res 2007; 13:1098-106.
32. Van Cutsem E, Kohne CH, Hitre E, et al. Cetuximab and chemotherapy as initial treatment for metastatic colorectal cancer. N Engl J Med 2009; 360:1408-17.
33. Marshall MV, Draney D, Sevick-Muraca EM, et al. Single-dose intravenous toxicity study of IRDye 800CW in Sprague-Dawley rats. Mol Imaging Biol 2010; 12:583-94.
34. Frangioni JV. Translating in vivo diagnostics into clinical reality. Nat Biotechnol 2006; 24:909-13.
35. Liersch T, Meller J, Kulle B, et al. Phase II trial of carcinoembryonic antigen radioimmunotherapy with 131I-labetuzumab after salvage resection of colorectal metastases in the liver: five-year safety and efficacy results. J Clin Oncol 2005; 23:6763-70.
36. Kraeber-Bodere F, Rousseau C, Bodet-Milin C, et al. Targeting, toxicity, and efficacy of 2-step, pretargeted radioimmunotherapy using a chimeric bispecific antibody and 131I-labeled bivalent hapten in a phase I optimization clinical trial. J Nucl Med 2006; 47:247-55.
37. Orcutt KD, Ackerman ME, Cieslewicz M, et al. A modular IgG-scFv bispecific antibody topology. Protein Eng Des Sel 2010; 23:221-8.
38. Frangioni JV. The problem is background, not signal. Mol Imaging 2009; 8:303-4.
39. Choi HS, Liu W, Liu F, et al. Design considerations for tumour-targeted nanoparticles. Nat Nanotechnol 2010; 5:42-7.
40. Goel A, Colcher D, Baranowska-Kortylewicz J, et al. Genetically engineered tetravalent single-chain Fv of the pancarcinoma monoclonal antibody CC49: improved biodistribution and potential for therapeutic application. Cancer Res 2000; 60:6964-71.
41. Lovdal T, Andersen E, Brech A, et al. Fc receptor mediated endocytosis of small soluble immunoglobulin G immune complexes in Kupffer and endothelial cells from rat liver. J Cell Sci 2000; 113:3255-66.
42. Mieog JS, Vahrmeijer AL, Hutteman M, et al. Novel intraoperative near-infrared fluorescence camera system for optical image-guided cancer surgery. Mol Imaging 2010; 9:223-31.

43. Beer AJ, Niemeyer M, Carlsen J, et al. Patterns of alphavbeta3 expression in primary and metastatic human breast cancer as shown by 18F-Galacto-RGD PET. J Nucl Med 2008; 49:255-9.
44. Wu Y, Cai W, Chen X. Near-infrared fluorescence imaging of tumor integrin alpha v beta 3 expression with Cy7-labeled RGD multimers. Mol Imaging Biol 2006; 8:226-36.
45. Coleman PJ, Brashear KM, Askew BC, et al. Nonpeptide alphavbeta3 antagonists. Part 11: discovery and preclinical evaluation of potent alphavbeta3 antagonists for the prevention and treatment of osteoporosis. J Med Chem 2004; 47:4829-37.
46. Keramidas M, Josserand V, Righini CA, et al. Intraoperative near-infrared image-guided surgery for peritoneal carcinomatosis in a preclinical experimental model. Br J Surg 2010; 97:737-43.
47. Hutteman M, Mieog JS, van der Vorst JR, et al. Intraoperative near-infrared fluorescence imaging of colorectal metastases targeting integrin alpha(v)beta(3) expression in a syngeneic rat model. Eur J Surg Oncol 2011; 37:252-7.
48. Kampmeier F, Niesen J, Koers A, et al. Rapid optical imaging of EGF receptor expression with a single-chain antibody SNAP-tag fusion protein. Eur J Nucl Med Mol Imaging 2010; 37:1926-34.